Supplementary Information

Deep Learning Dynamic Allostery of G-Protein-Coupled Receptors

Hung N. Do[1], Jinan Wang[1], and Yinglong Miao[1,*]

[1]Center for Computational Biology and Department of Molecular Biosciences, University of Kansas, Lawrence, Kansas 66047

*To whom correspondence should be addressed: miao@ku.edu

Supplementary Figure 1. Time courses of the RMSDs of orthosteric ligands and NAMs relative to the respective starting structures calculated from GaMD simulations of class A GPCRs in the (A) M_1R without and with MT7, **(B)** β_2AR without and with Cmpd-15, **(C)** β_2AR without and with AS408, **(D)** C5AR1 without and with NDT9513727, **(E)** C5AR1 without and with Avacopan, **(F)** CB1 without and with ORG27569, and **(G)** CCR2 without and with GTPL9431. From left to right for each system are the RMSDs of the orthosteric ligand in the absence and presence of NAM (denoted "Antagonist" or "Agonist" and "AntagonistNAM" or "AgonistNAM", respectively) and RMSD of the NAM. The averages and standard deviations of the ligand RMSDs were included in each panel in the parentheses.

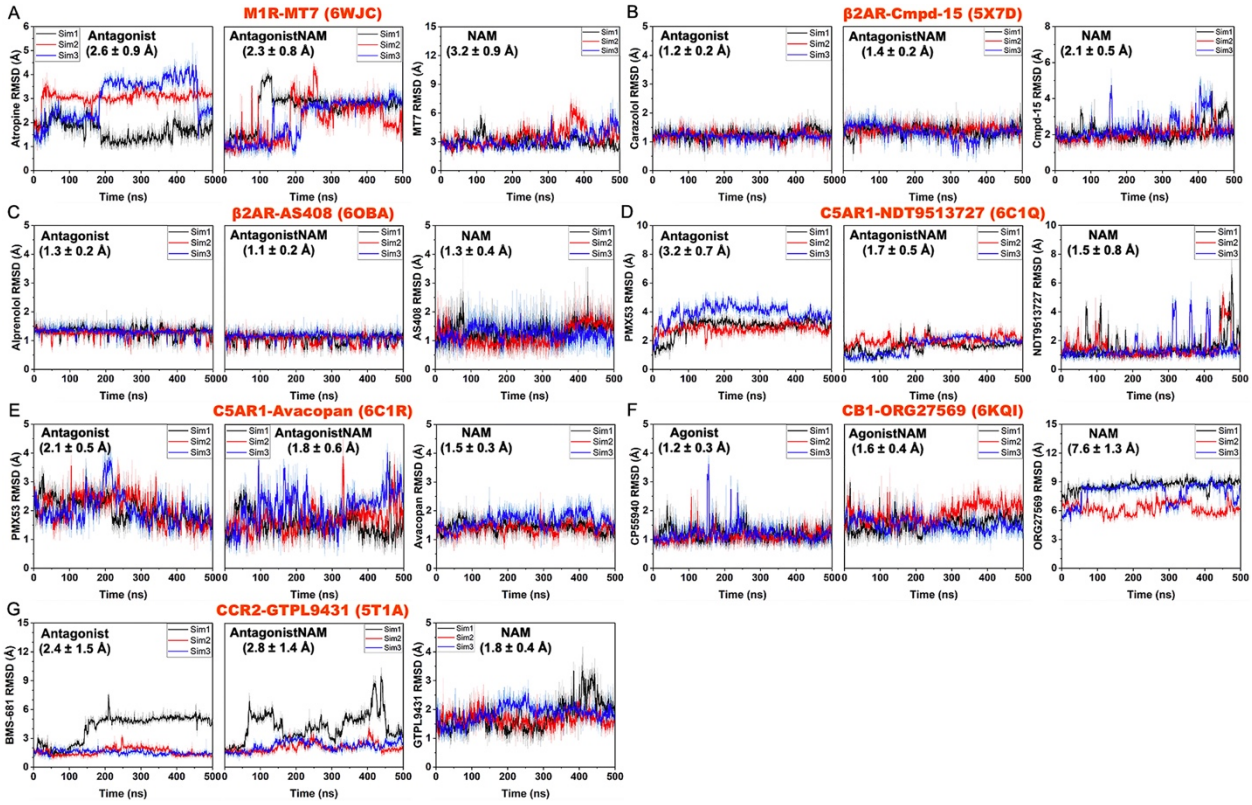

Supplementary Figure 2. Time courses of the RMSDs of orthosteric ligands and PAMs relative to the respective starting structures calculated from GaMD simulations of class A GPCRs in the (A) A_1AR without and with MIPS521, **(B)** M_2R without and with LY2119620, **(C)** M_4R without and with LY2119620, **(D)** β_2AR without and with Cmpd-6FA, **(E)** D_1R without and with LY3154207, **(F)** FFAR1 without and with AgoPAM, and **(G)** GPBAR without and with INT777. From left to right for each system are the RMSDs of the orthosteric ligand in the absence and presence of PAM (denoted "Agonist" and "AgonistNAM", respectively) and RMSDs of the PAM. The averages and standard deviations of the ligand RMSDs were included in each panel in the parentheses.

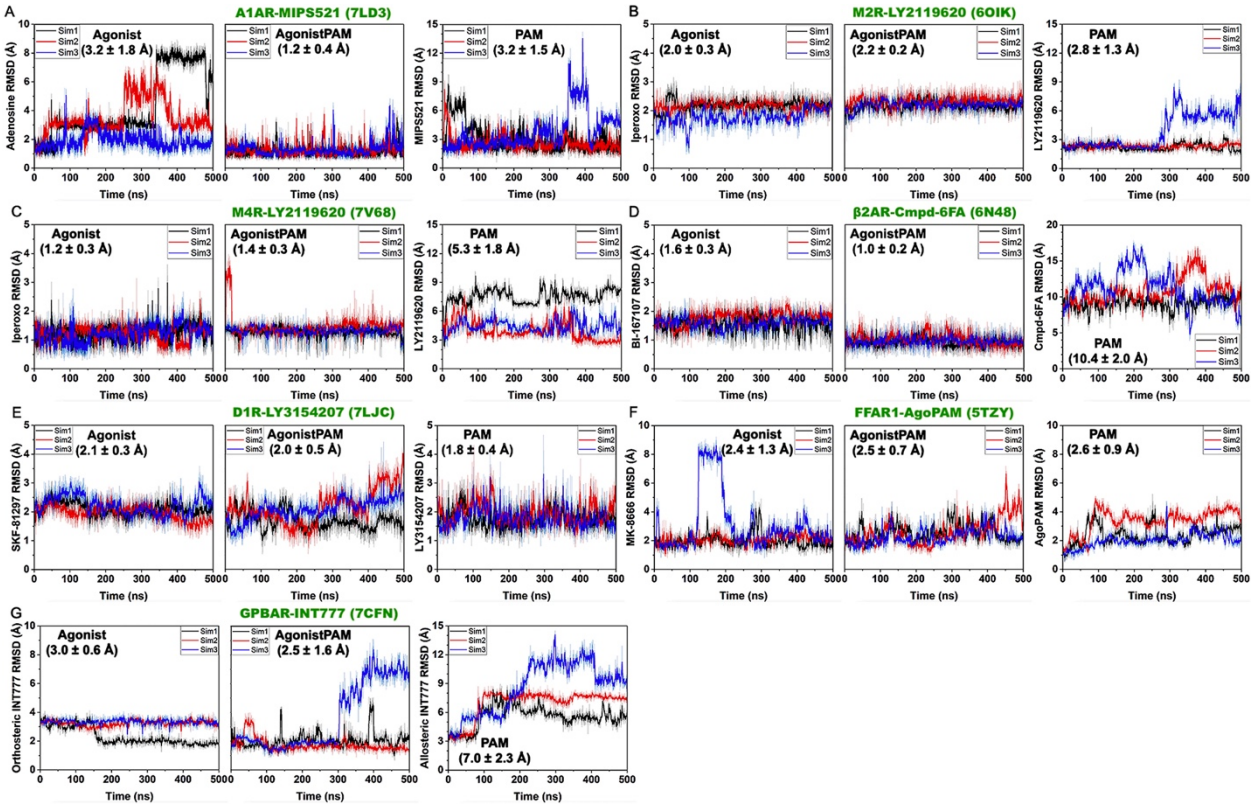

Supplementary Figure 3. Time courses of the RMSDs of orthosteric and allosteric ligands relative to the respective starting structures calculated from GaMD simulations of class B GPCRs in the (A) GLP1R with the NNC0640 NAM, **(B)** GLP1R with the PF-06372222 NAM, **(C)** GLP1R without and with the LSN3160440 PAM, and **(D)** GLR with the MK-0893 NAM. From left to right for **(C)** and **(D)** are the RMSDs of orthosteric ligands in the absence and presence of allosteric ligands (denoted "Agonist" or "Antagonist" and "AgonistPAM" or "AntagonistNAM", respectively) and RMSDs of allosteric ligands. The averages and standard deviations of the ligand RMSDs were included in each panel in the parentheses.

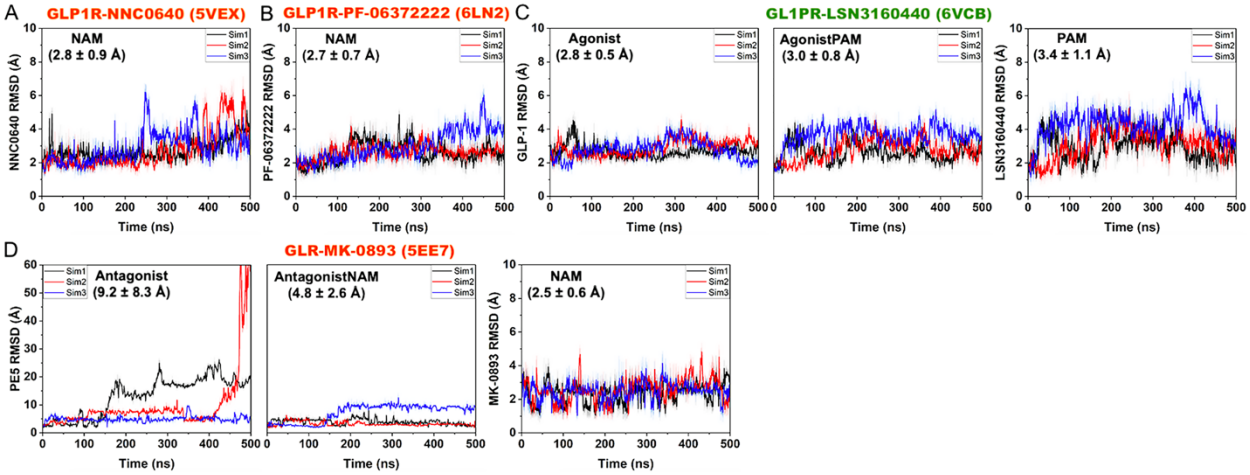

Supplementary Figure 4. Changes in root-mean-square fluctuations (RMSFs) of receptors and orthosteric ligands of class A and B GPCRs upon binding of NAMs calculated from GaMD simulations of the MT7-bound M_1R (PDB: 6WJC) **(A)**, Cmpd-15-bound β_2AR (PDB: 5X7D) **(B)**, AS408-bound β_2AR (PDB: 6OBA) **(C)**, NDT9513727-bound C5AR1 (PDB: 6C1Q) **(D)**, Avacopan-bound C5AR1 (PDB: 6C1R) **(E)**, ORG27569-bound CB_1 (PDB: 6KQI) **(F)**, GTPL9431-bound CCR2 (PDB: 5T1A) **(G)**, NNC0640-bound GLP1R (PDB: 5VEX) **(H)**, PF-06372222-bound GLP1R (PDB: 6LN2) **(I)**, and MK-0893-bound GLR (PDB: 5EE7) **(J)**. A color scale of -1.0 (blue) to 0 (white) to 1.0 (red) is used to show the changes in RMSFs, and NAMs are colored orange.

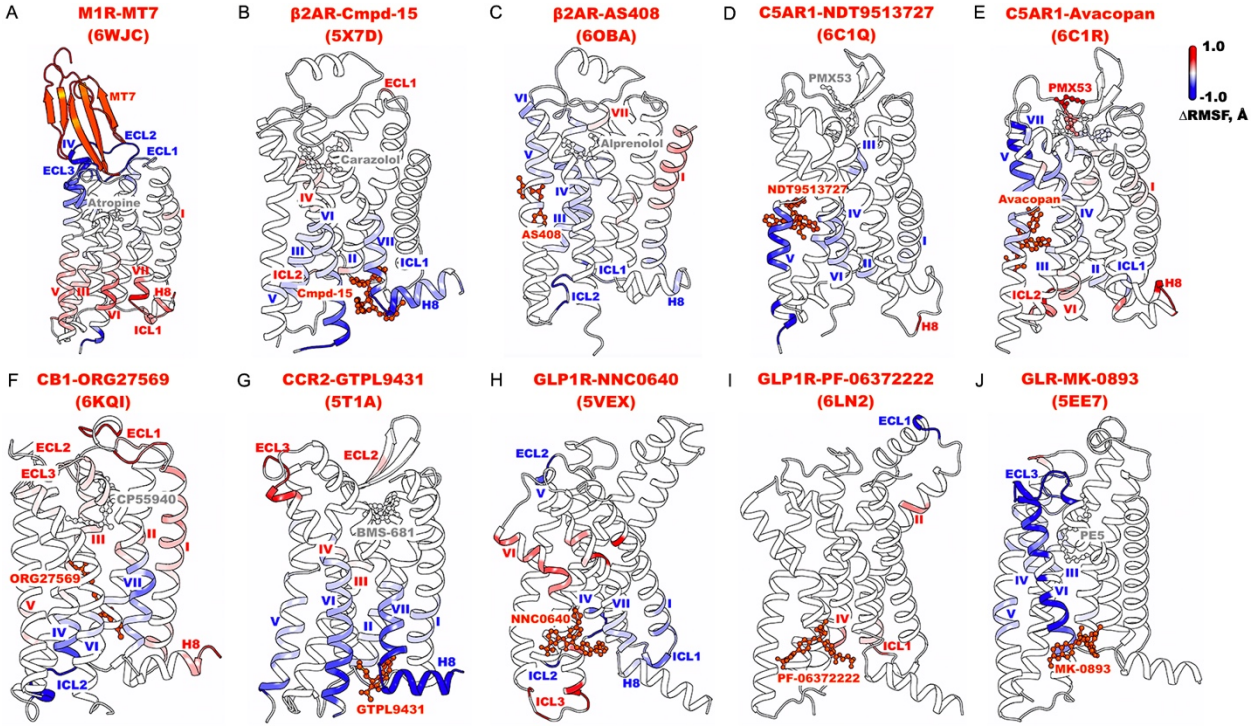

Supplementary Figure 5. Changes in root-mean-square fluctuations (RMSFs) of receptors and orthosteric ligands of class A and B GPCRs upon binding of PAMs calculated from GaMD simulations of the MIPS521-bound A_1AR (PDB: 7LD3) **(A)**, LY2119620-bound M_2R (PDB: 6OIK) **(B)**, LY2119620-bound M_4R (PDB: 7V68) **(C)**, Cmpd-6FA-bound β_2AR (PDB: 6N48) **(D)**, LY3154207-bound D_1R (PDB: 7LJC) **(E)**, AgoPAM-bound FFAR1 (PDB: 5TZY) **(F)**, INT777-bound GPBAR (PDB: 7CFN) **(G)**, and LSN3160440-bound GLP1R **(H)**. A color scale of -1.0 (blue) to 0 (white) to 1.0 (red) is used to show the changes in RMSFs, and PAMs are colored green.

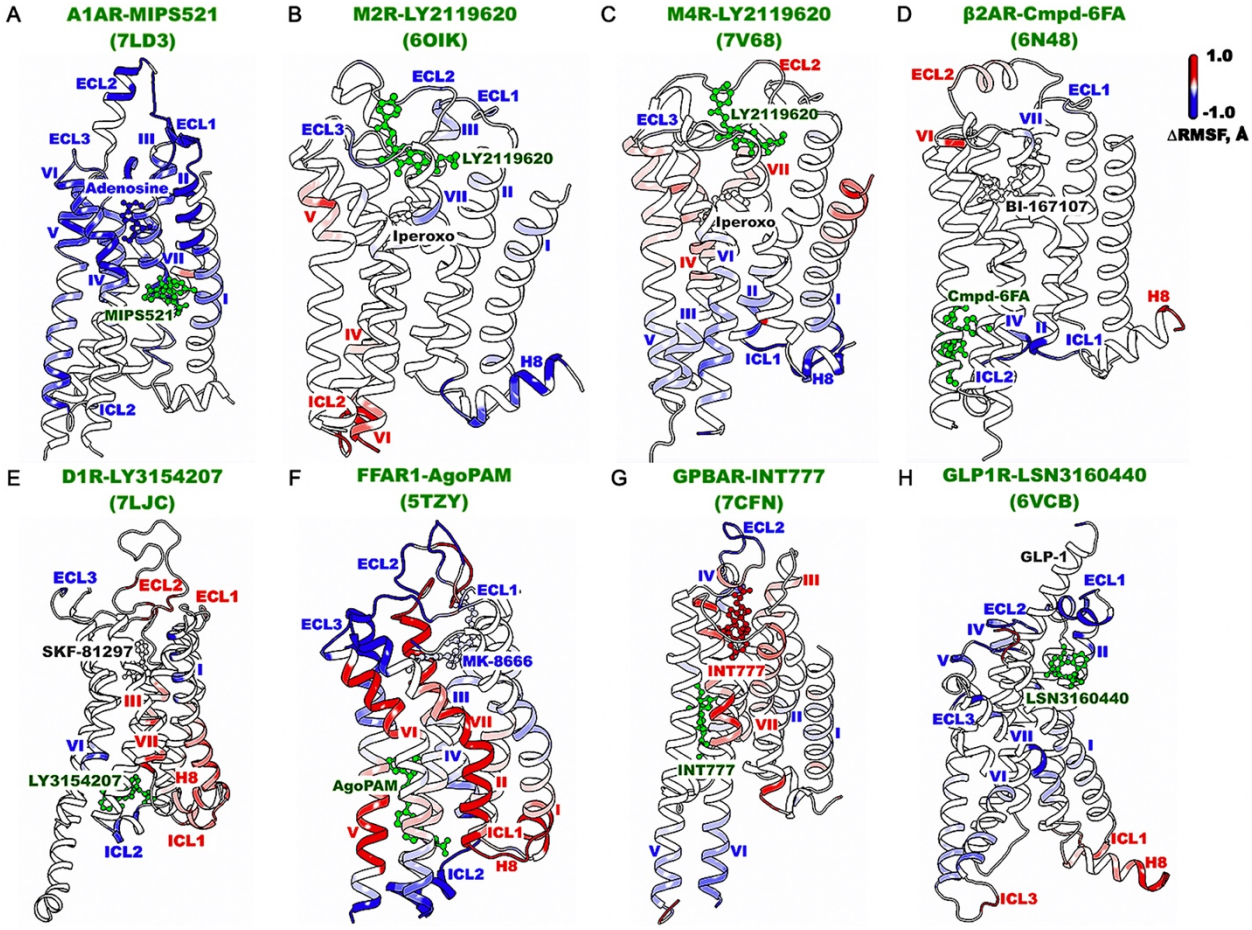

Supplementary Figure 6. Accuracy curves of the training and validation datasets for GPCR allosteric modulation of the A_1AR **(A)**, muscarinic receptors M_1R, M_2R and M_4R **(B)**, β_2AR **(C)**, C5AR1 **(D)**, CB_1 **(E)**, CCR2 **(F)**, D_1R **(G)**, FFAR1 **(H)**, GPBAR **(I)**, GLP1R **(J)**, and GLR **(K)**.

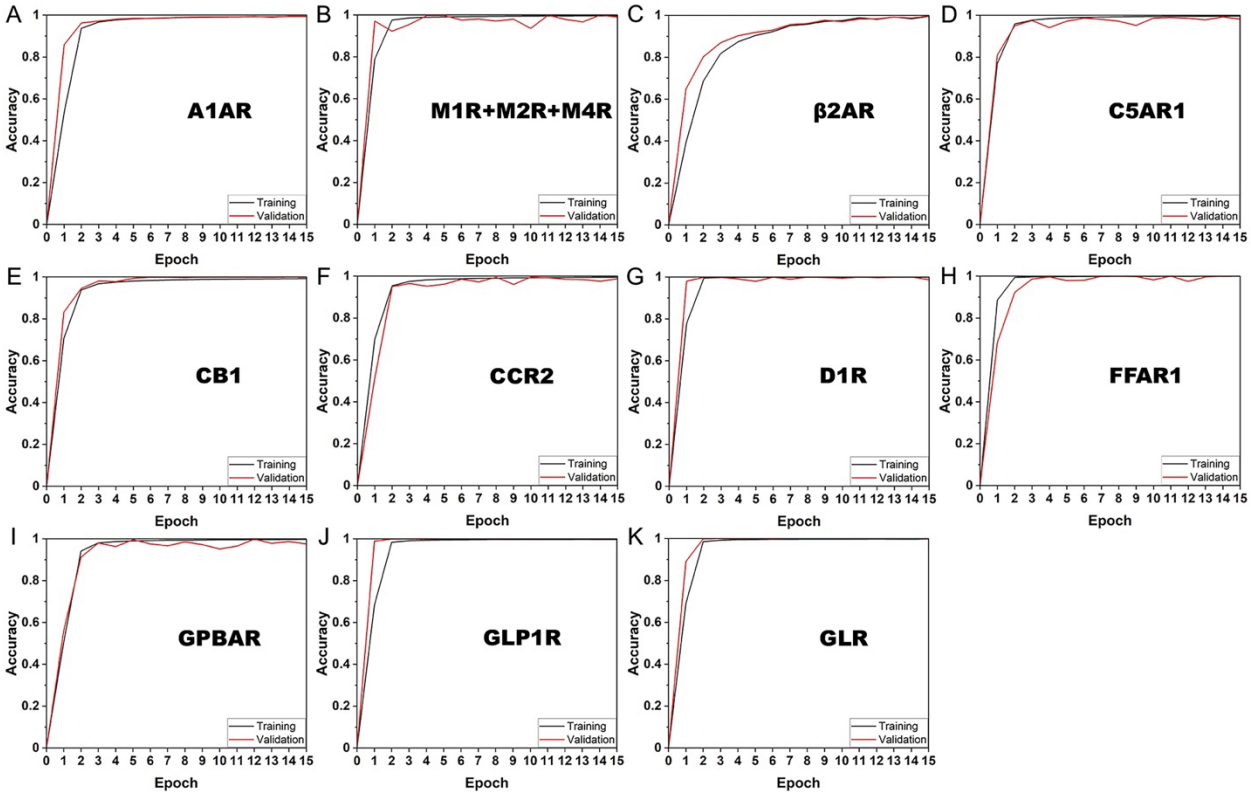

Supplementary Figure 7. Confusion matrices calculated from the validation datasets for GPCR allosteric modulation of the A_1AR **(A)**, muscarinic receptors M_1R, M_2R and M_4R **(B)**, β_2AR **(C)**, C5AR1 **(D)**, CB_1 **(E)**, CCR2 **(F)**, D_1R **(G)**, FFAR1 **(H)**, GPBAR **(I)**, GLP1R **(J)**, and GLR **(K)**.

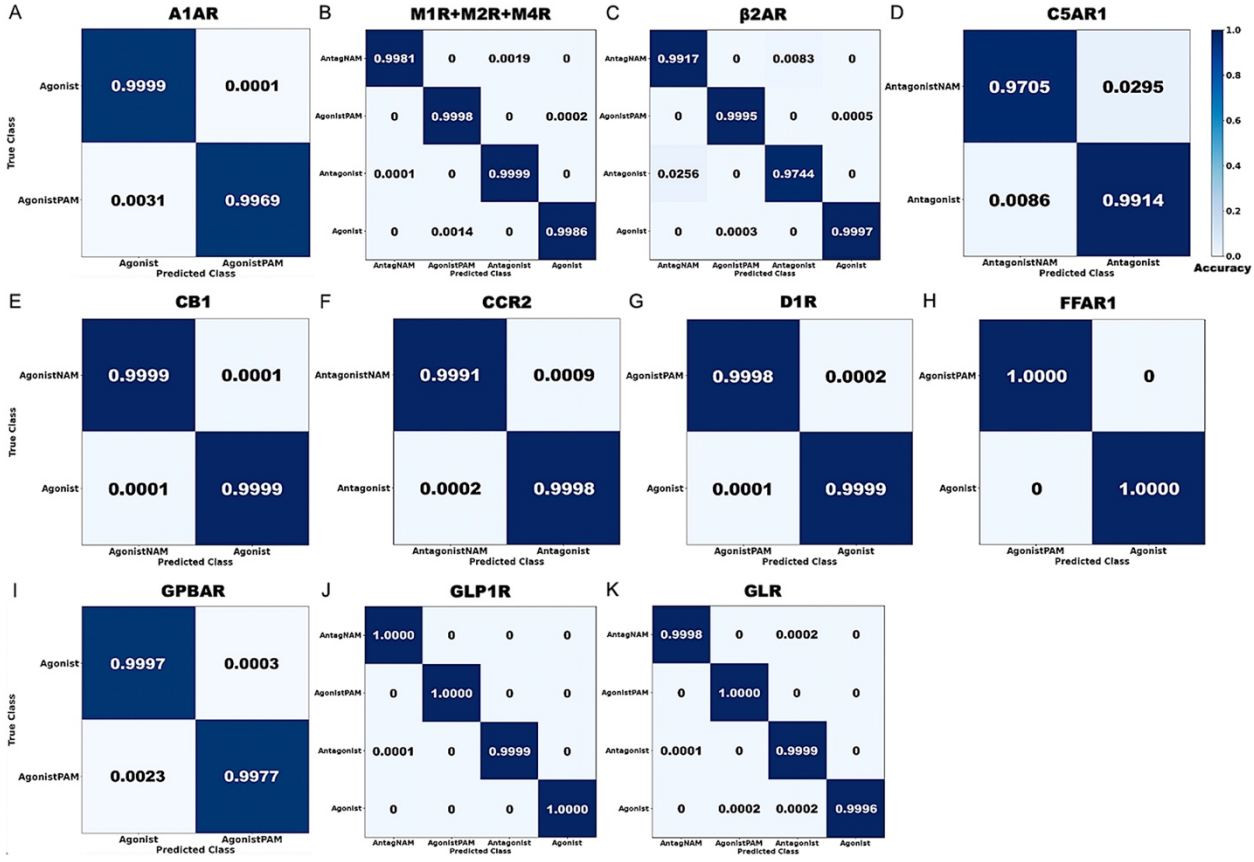

Supplementary Figure 8. Saliency (attention) maps of residue contact gradients of class A and B GPCRs bound by negative allosteric modulators (NAMs), including the MT7-bound M_1R (PDB: 6WJC) **(A)**, Cmpd-15-bound β_2AR (PDB: 5X7D) **(B)**, AS408-bound β_2AR (PDB: 6OBA) **(C)**, NDT9513727-bound C5AR1 (PDB: 6C1Q) **(D)**, Avacopan-bound C5AR1 (PDB: 6C1R) **(E)**, ORG27569-bound CB_1 (PDB: 6KQI) **(F)**, GTPL9431-bound CCR2 (PDB: 5T1A) **(G)**, NNC0640-bound GLP1R (PDB: 5VEX) **(H)**, PF-06372222-bound GLP1R (PDB: 6LN2) **(I)**, and MK-0893-bound GLR (PDB: 5EE7) **(J)**. The seven transmembrane (TM) helices are labeled I-VII. Regions that contain residue contacts selected for free energy profiling are boxed in blue color. The gradients of residue contacts are shown in a 0.2 (white) to 0.25 (black) color scale.

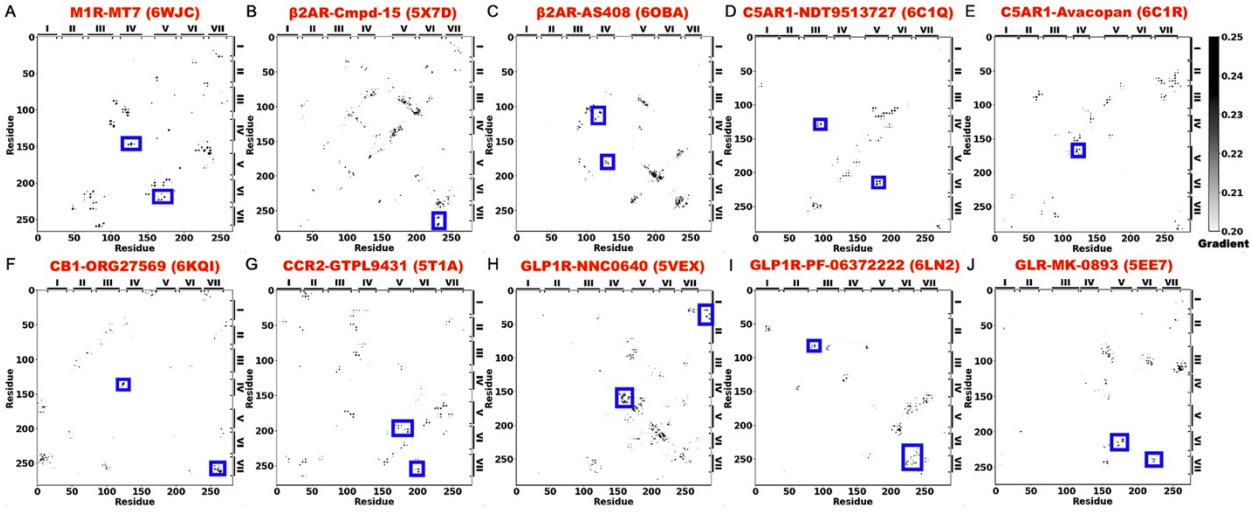

Supplementary Figure 9. Saliency (attention) maps of residue contact gradients of class A and B GPCRs bound by positive allosteric modulators (PAMs), including the MIPS521-bound A_1AR (PDB: 7LD3) **(A)**, LY2119620-bound M_2R (PDB: 6OIK) **(B)**, LY2119620-bound M_4R (PDB: 7V68) **(C)**, Cmpd-6FA-bound β_2AR (PDB: 6N48) **(D)**, LY3154207-bound D_1R (PDB: 7LJC) **(E)**, AgoPAM-bound FFAR1 (PDB: 5TZY) **(F)**, INT777-bound GPBAR (PDB: 7CFN) **(G)**, and LSN3160440-bound GLP1R **(H)**. The seven TM helices are labeled I-VII. Regions that contain residue contacts selected for free energy profiling are boxed in blue color. The gradients of residue contacts are shown in a 0.2 (white) to 0.25 (black) color scale.

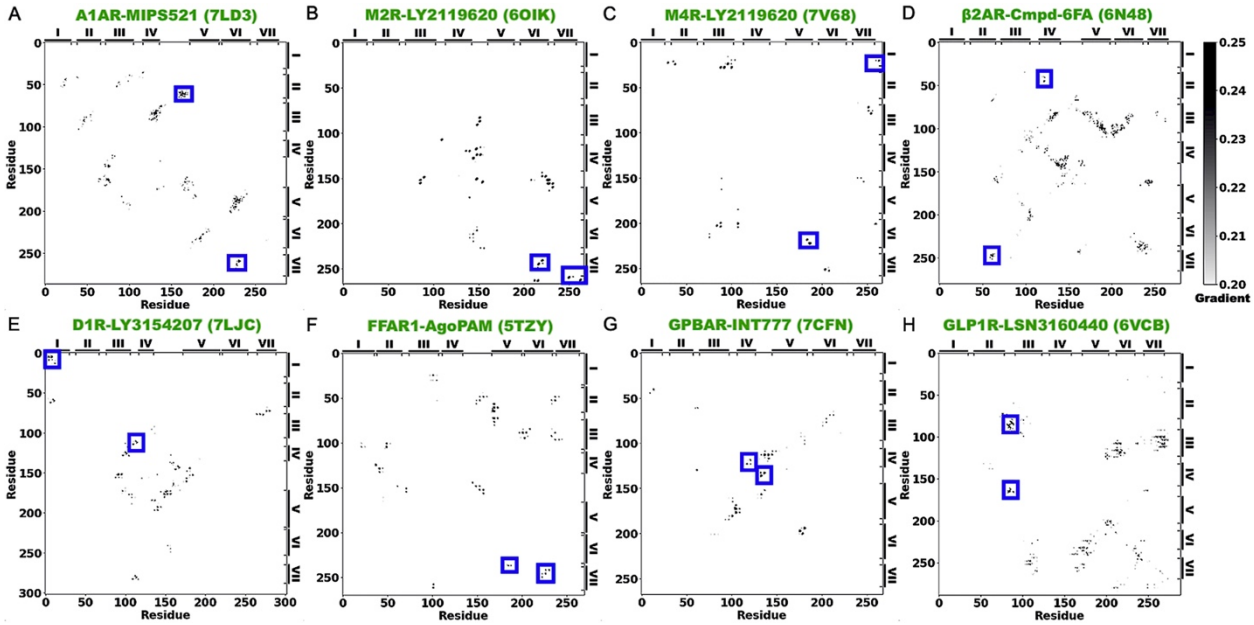

Supplementary Figure 10. Reduced binding preference of NAMs (MT7 and Cmpd-15) and PAMs (LY2119620 and LY3154207) to "non-cognate" GPCRs. (A-C) 2D free energy profiles of the heavy-atom RMSDs of the atropine antagonist and C_α-atom RMSDs of the MT7 NAM relative to their starting structures in the M_1R (PDB: 6WJC) **(A)**, model M_2R **(B)**, and model M_4R **(C)** bound by MT7. **(D-H)** 2D free energy profiles of the heavy-atom RMSDs of the carazolol antagonist and Cmpd-15 NAM relative to their starting structures in the β_2AR (PDB: 5X7D) **(D),** model $\alpha_{1B}AR$ **(E)**, model $\alpha_{2A}AR$ **(F)**, model $\alpha_{2C}AR$ **(G)**, and model β_1AR **(H)** bound by Cmpd-15. **(I-K)** 2D free energy profiles of the heavy-atom RMSDs of the iperoxo agonist and LY2119620 PAM relative to their starting structures in the M_2R (PDB: 6OIK) **(I)**, M_4R (PDB: 7V68) **(J)**, and model M_1R **(K)** bound by LY2119620. **(L-M)** 2D free energy profiles of the heavy-atom RMSDs of the SKF-81297 agonist and LY3154207 PAM relative to their starting structures in the D_1R (PDB: 7LJC) **(L)** and model D_2R **(M)** bound by LY3154207.

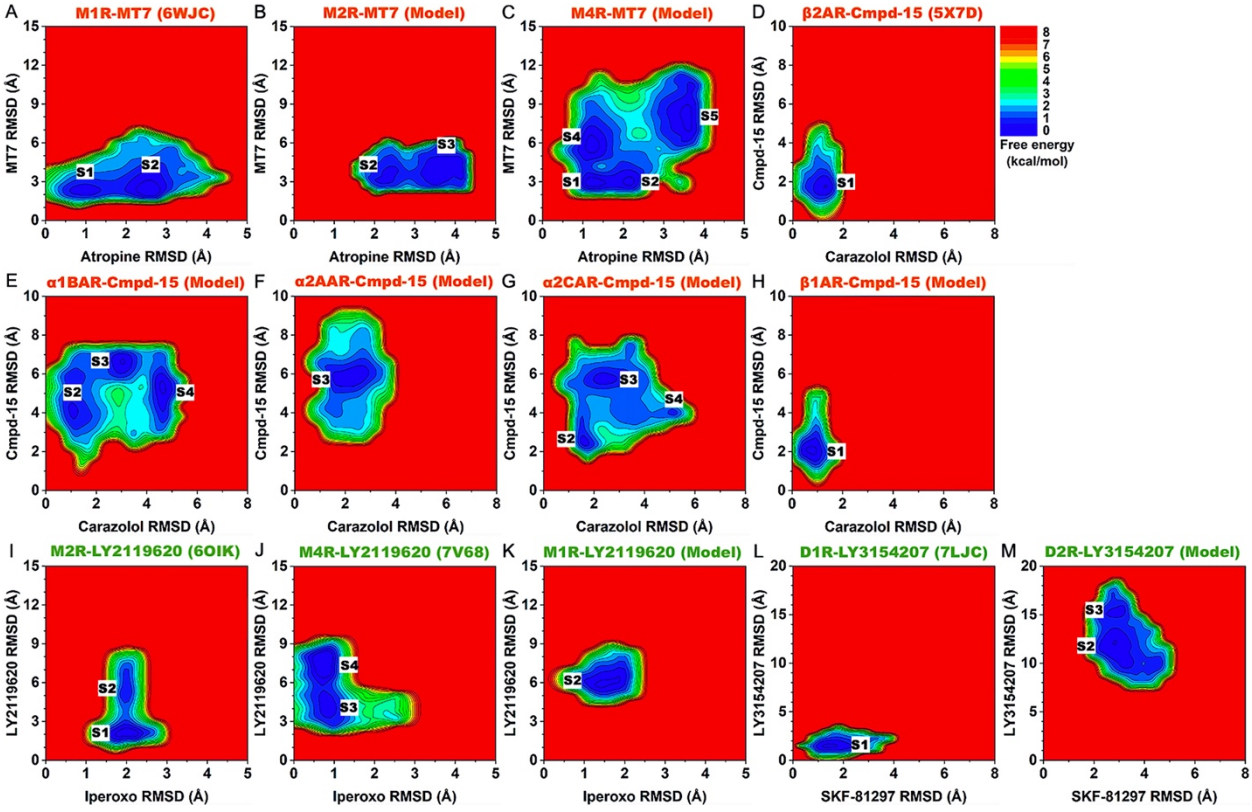

Supplementary Table 1. Summary of GaMD simulations performed on the PDB structures and computational models ("Model") of GPCRs with and without the positive/negative allosteric modulator (PAM/NAM). **(a)** PDB IDs or computational models ("Model") built for GaMD simulations. **(b)** Types of modulators bound in GPCRs. **(c)** Names and overall charges of orthosteric ligands bound in GPCRs. **(d)** Names and overall charges of allosteric ligands bound in GPCRs. **(e)** Averages and standard deviations of boost potentials ΔV (kcal/mol) calculated from three independent 500ns GaMD simulations for each GPCR system.

Receptor	PDB/Model[a]	PAM/NAM[b]	Orthosteric ligand (charge)[c]	Allosteric ligand (charge)[d]	ΔV (kcal/mol) (3 x 500ns)[e]
A_1AR	7LD3	PAM	Adenosine (0)	MIPS521 (0)	20.3 ± 7.2
				-	19.0 ± 8.0
M_1R	6WJC	NAM	Atropine (0)	MT7 (0)	13.1 ± 4.1
				-	14.3 ± 4.3
	Model	PAM	Iperoxo (+1)	LY2119620 (0)	15.4 ± 4.5
M_2R	Model	NAM	Atropine (0)	MT7 (0)	14.0 ± 4.2
	6OIK	PAM	Iperoxo (+1)	LY2119620 (0)	14.0 ± 4.3
				-	15.0 ± 4.5
M_4R	Model	NAM	Atropine (0)	MT7 (0)	13.8 ± 4.2
	7V68	PAM	Iperoxo (+1)	LY2119620 (0)	14.6 ± 4.4
				-	15.3 ± 4.8
$\alpha_{1B}AR$	Model	NAM	Carazolol (+1)	Cmpd-15 (0)	13.9 ± 4.2
$\alpha_{2A}AR$	Model	NAM	Carazolol (+1)	Cmpd-15 (0)	14.0 ± 4.3
$\alpha_{2C}AR$	Model	NAM	Carazolol (+1)	Cmpd-15 (0)	14.4 ± 4.3
β_1AR	Model	NAM	Carazolol (+1)	Cmpd-15 (0)	14.4 ± 4.3
β_2AR	5X7D	NAM	Carazolol (+1)	Cmpd-15 (0)	14.5 ± 4.3
				-	14.3 ± 4.3
	6OBA	NAM	Alprenolol (+1)	AS408 (+1)	14.4 ± 4.3
				-	14.7 ± 4.4
	6N48	PAM	BI-167107 (+1)	Cmpd-6FA (-1)	14.3 ± 4.3
				-	14.5 ± 4.3
C5AR1	6C1Q	NAM	PMX53 (0)	NDT9513727 (0)	13.8 ± 4.2
				-	14.2 ± 4.3
	6C1R	NAM	PMX53 (0)	Avacopan (0)	13.2 ± 4.1
				-	14.4 ± 4.3
CB_1	6KQI	NAM	CP55940 (0)	ORG27569 (0)	13.0 ± 4.1
				-	13.6 ± 4.2
CCR2	5T1A	NAM	BMS-681 (0)	GTPL9431 (0)	13.9 ± 4.2
				-	13.6 ± 4.2
D_1R	7LJC	PAM	SKF-81297 (+1)	LY3154207 (0)	13.3 ± 4.2
				-	14.6 ± 4.4
D_2R	Model	PAM	SKF-81297 (+1)	LY3154207 (0)	15.2 ± 4.5
FFAR1	5TZY	PAM	MK-8666 (-1)	AgoPAM (-1)	13.8 ± 4.2
				-	14.1 ± 4.3
GPBAR	7CFN	PAM	INT777 (-1)	INT777 (-1)	14.3 ± 4.3
				-	15.3 ± 4.5
GLP1R	5VEX	NAM	-	NNC0640 (0)	14.0 ± 4.3
				-	14.4 ± 4.4
	6LN2	NAM	-	PF-06372222 (-1)	14.2 ± 4.3
				-	14.5 ± 4.3
	6VCB	PAM	GLP-1 (0)	LSN3160440 (+1)	13.4 ± 4.2
				-	15.8 ± 4.6
GLR	5EE7	NAM	PE5 (0)	MK-0893 (-1)	13.7 ± 4.3
				-	15.0 ± 4.4

Supplementary Table 2. Characteristic residue contacts with ≥ 0.7 gradients identified from GLOW analysis of GPCR allosteric modulation. Residue contacts selected for free energy profiling are in bold.

System	PDB/Model	PAM/NAM	Residue contacts
A_1AR-MIPS521	7LD3	PAM	T23.52^{ECL1} – P165^{ECL2}, N2.65 – C45.50^{ECL2}, C3.25 – K168^{ECL2}, Q23.51^{ECL1} – C45.50^{ECL2}, Y5.58 – F6.42, L5.53 – S6.47, **G2.68 – K168^{ECL2},** E5.36 – L6.59, **W6.48 – L7.41,** N148^{ECL2} – V152^{ECL2}
M_1R-MT7	6WJC	NAM	**V4.68 – T172^{ECL2}, P5.36 – T6.59**, W4.64 – Q177^{ECL2}
M_2R-LY2119620	6OIK	PAM	G3.21 – D173^{ECL2}, P34.50^{ICL2} – K34.56^{ICL2}, V6.33 – N8.47, V168^{ECL2} – D173^{ECL2}, **M6.54 – G7.38,** P3.22 – D173^{ECL2}, **C7.56 – T8.49,** T8.53 – L8.57
M_4R-LY2119620	7V68	PAM	**N1.60 – T8.53, S5.62 – T6.34,** N1.60 – L12.50^{ICL1}, N1.60 – T2.37, P5.36 – T6.59, I6.40 – Y7.53
β_2AR-Cmpd-15	5X7D	NAM	K34.52^{ICL2} – K6.29, D3.49 – K6.29, R12.49^{ICL1} – D8.49, E6.30 – R7.55, **T6.36 – I7.52, K6.29 – P8.48**
β_2AR-AS408	6OBA	NAM	S34.55^{ICL2} – T4.38, Y34.53^{ICL2} – L34.56^{ICL2}, **T4.56 – V5.45, L34.56^{ICL2} – I4.45,** V3.33 – F4.58, E3.41 – V5.46, C6.27 – A6.33, E3.41 – S4.53
β_2AR-Cmpd-6FA	6N48	PAM	**T2.39 – K4.39**, H178^{ECL2} – N183^{ECL2}, **K2.68 – E7.33**, R3.50 – L6.34, A3.38 – W6.48, F45.52^{ECL2} – L302^{ECL3}, R3.50 – F5.62, L34.56^{ICL2} – I4.45
C5AR1-NDT9513727	6C1Q	NAM	N34.55^{ICL2} – S5.67, F3.55 – G4.40, N3.35 – N7.45, **T3.45 – A4.45, L5.51 – F6.45**, S3.26 – V7.39
C5AR1-Avacopan	6C1R	NAM	I2.59 – D7.35, Y4.63 – K5.32, R4.64 – R5.42, L3.43 – I7.51, **L4.56 – L5.45, P4.59 – V5.38**
CB_1-ORG27569	6KQI	NAM	F102 – V7.34, V110 – D266^{ECL2}, M103 – D266^{ECL2}, V110 – T7.33, L12.50^{ICL1} – L8.50, **R34.55^{ICL2} – T4.38,** I6.40 – I7.52, **T7.47 – L7.55**
CCR2-GTPL9431	5T1A	NAM	V6.43 – N7.49, **I5.61 – K6.28, V6.36 – V7.56**, W5.34 – F6.64, P5.50 – W6.48, I3.54 – R5.63, W5.34 – N276^{ECL3}, L34.54^{ICL2} – R34.57^{ICL2}, R34.57^{ICL2} – S5.62
D_1R-LY3154207	7LJC	PAM	S172^{ECL2} – E181^{ECL2}, N3.26 – S45.52^{ECL2}, K167^{ECL2} – R5.36, P34.50^{ICL2} – F7.55, V1.31 – E2.65, **P34.50^{ICL2} – K34.56^{ICL2}, V1.31 – I1.43**, W163^{ECL2} – N185^{ECL2}
FFAR1-AgoPAM	5TZY	PAM	**P5.32 – N252^{ECL3}, P34.50^{ICL2} – F34.56^{ICL2},** S6.54 – W7.34, G6.39 – V7.52, S154^{ECL2} – T162^{ECL2}, R3.50 – T7.53, L3.43 – S7.45, G70^{ECL1} – L45.51^{ECL2}
GPBAR-INT777	7CFN	PAM	I1.47 – L2.51, G4.63 – G152^{ECL2}, W149^{ECL2} – G152^{ECL2}, G152^{ECL2} – A159^{ECL2}, **W149^{ECL2} – N154^{ECL2}**, L5.69 – T6.30, I1.47 – L2.51, **L4.59 – G4.63,** P151^{ECL2} – A5.36
GLP1R-NNC0640	5VEX	NAM	I1.60 – C7.58, **L12.49^{ICL1} – V8.50, E4.38 – W4.40,** N5.32 – N5.34, N300^{ECL2} – W5.36, Q210^{ECL1} – W45.51^{ECL2}, L6.48 – T7.46, L6.38 – L7.56
GLP1R-PF-06372222	6LN2	NAM	S219^{ECL1} – L3.31, Y220^{ECL1} – C45.50^{ECL2}, Y1.40 – D2.68, T2.45 – Q4.39, **Q210^{ECL1} – H212^{ECL1}, L6.49 – Q7.49**
GLP1R-LSN3160440	6VCB	PAM	F5.54 – I6.46, **A208^{ECL1} – L217^{ECL1}, Q221^{ECL1} – E294^{ECL2}**, Y3.45 – F7.40, R5.40 – I6.46, L3.47 – Y7.57
GLR-MK-0893	5EE7	NAM	K4.64 – N291^{ECL2}, N298^{ECL2} – K7.38, G3.39 – K7.38, V3.34 – W5.36, **F5.51 – I6.46, D6.61 – R7.35**

Supplementary Table 3. Summary of the 2D free energy profiles of characteristic residues in the allosteric modulation of class A and B GPCRs bound by NAMs in Figure 4. Locations of the energy minima are included in the third and last columns, with coordinates of the first and second reaction coordinates listed.

System	Reaction coordinates	Without NAM	With NAM
M_1R-MT7	V4.68-T172 Distance, P5.36-T6.59 Distance	**S1**(~9.0Å, ~4.5Å) **S2**(~11.9Å, ~4.6Å)	**S1**(~9.5Å, ~5Å)
β_2AR-Cmpd-15	T6.36-I7.52 Distance, K6.29-P8.48 Distance	**S1**(~6.7Å, ~6.5Å) **S2**(~6.7Å, ~10.0Å) **S3**(~7.5Å, ~11.0Å)	**S3**(~7.0Å, ~10.0Å)
β_2AR-AS408	T4.56-V5.45 Distance, L34.56^{ICL2}-I4.45 Distance	**S1**(~8.0Å, ~12.5Å) **S2**(~7.2Å, ~8.0Å)	**S1**(~8.0Å, ~12.5Å)
C5AR1-NDT9513727	T3.45-A4.45 Distance, L5.51-F6.45 Distance	**S1**(~7.0Å, ~7.0Å) **S2**(~7.0Å, ~10.5Å)	**S1**(~7.5Å, ~7.5Å)
C5AR1-Avacopan	L4.56-L5.45 Distance, P4.59-V5.38 Distance	**S1**(~9.0Å, ~7.0Å) **S2**(~11.8Å, ~11.0Å)	**S1**(~8.5Å, ~6.5Å)
CB1-ORG27569	R34.55^{ICL2}-T4.38 Distance, T7.47-L7.55 RMSD	**S1**(~6.0Å, ~0.5Å)	**S1**(~6.0Å, ~0.5Å)
CCR2-GTPL9431	I5.61-K6.28 Distance, V6.36-V7.56 Distance	**S1**(~7.5Å, ~6.5Å)	**S1**(~5.0Å, ~6.3Å)
GLP1R-NNC0640	L12.49^{ICL1}-V8.50 Distance, E4.38-W4.40 RMSD	**S1**(~7.5Å, ~2.0Å)	**S1**(~7.5Å, ~1.5Å)
GLP1R-PF-06372222	Q210^{ECL1}-H212^{ECL1} RMSD, L6.49-Q7.49 Distance	**S1**(~5.0Å, ~6.5Å)	**S1**(~2.5Å, ~7.5Å)
GLR-MK-0893	F5.51-I6.46 Distance, D6.61-R7.35 Distance	**S1**(~7.0Å, ~9.0Å) **S2**(~7.5Å, ~12.0Å) **S3**(~11.9Å, ~8.5Å)	**S1**(~7.5Å, ~9.5Å)

Supplementary Table 4. Summary of the 2D free energy profiles of characteristic residues in the allosteric modulation of class A and B GPCRs bound by PAMs in Figure 5. Locations of the energy minima are included in the third and last columns, with coordinates of the first and second reaction coordinates listed.

System	Reaction coordinates	Without PAM	With PAM
A_1AR-MIPS521	G2.68-K168^{ECL2} Distance, W6.48-L7.41 Distance	**S1**(~8.0Å, ~7.5Å) **S2**(~5.5Å, ~10.0Å) **S3**(~11.5Å, ~10.0Å)	**S1**(~5.5Å, ~7.0Å)
M_2R-LY2119620	M6.54-G7.38 Distance, C7.56-T8.49 Distance	**S1**(~8.0Å, ~9.0Å)	**S1**(~8.0Å, ~9.0Å)
M_4R-LY2119620	N1.60-T8.53 Distance, S5.62-T6.34 Distance	**S1**(~10.0Å, ~5.5Å) **S2**(~6.0Å, ~5.5Å) **S3**(~11.0Å, ~8.0Å)	**S1**(~7.0Å, ~5.5Å)
β_2AR-Cmpd-6FA	T2.39-K4.39 Distance, K6.28-E7.33 Distance	**S1**(~9.0Å, ~12.0Å) **S2**(~15.5Å, ~11.5Å) **S3**(~12.5Å, ~7.5Å)	**S1**(~9.5Å, ~12.0Å)
D_1R-LY3154207	V1.31-I1.43 RMSD, P34.50^{ICL2}-K34.56^{ICL2} RMSD	**S1**(~2.0Å, ~2.5Å) **S2**(~5.0Å, ~2.0Å)	**S1**(~2.0Å, ~1.0Å)
FFAR1-AgoPAM	P5.32-N252 Distance, P34.50^{ICL2}-F34.56^{ICL2} Distance	**S1**(~7.0Å, ~9.5Å) **S2**(~14.0Å, ~13.0Å) **S3**(~13.0Å, ~8.5Å)	**S1**(~7.0Å, ~9.5Å)
GPBAR-INT777	L4.59-G4.63 RMSD, W149^{ECL2}-N154^{ECL2} Distance	**S1**(~2.0Å, ~3.0Å) **S2**(~3.0Å, ~10.0Å) **S3**(~7.0Å, ~5.0Å)	**S1**(~2.0Å, ~3.5Å) **S2**(~3.0Å, ~8.0Å)
GLP1R-LSN3160440	A208^{ECL1}-L217^{ECL1} Distance, Q221^{ECL1} – E294^{ECL2} Distance	**S1**(~5.5Å, ~7.5Å) **S2**(~7.5Å, ~8.0Å)	**S1**(~5.5Å, ~7.5Å)

Supplementary Table 5. Summary of the 2D free energy profiles of orthosteric and allosteric ligand binding in the M_1R, M_2R, and M_4R bound by the MT7 NAM, β_2AR, $\alpha_{1B}AR$, $\alpha_{2A}AR$, $\alpha_{2C}AR$, and β_1AR bound by the Cmpd-15 NAM, M_2R, M_4R, and M_1R bound by the LY2119620 PAM, and D_1R and D_2R bound by the LY3154207 PAM in Figure S10. Locations of the energy minima are included in the third and last columns, with coordinates of the first and second reaction coordinates listed.

System	Reaction coordinates	Low-energy states
M_1R-MT7	Atropine RMSD, MT7 RMSD	**S1**(~1.0Å, ~2.5Å) **S2**(~2.5Å, ~2.5Å)
M_2R-MT7		**S2**(~2.3Å, ~3.5Å) **S3**(~3.8Å, ~4.0Å)
M_4R-MT7		**S1**(~1.3Å, ~3.0Å) **S2**(~2.3Å, ~3.0Å) **S4**(~1.3Å, ~6.0Å) **S5**(~3.5Å, ~8.0Å)
β_2AR-Cmpd-15	Carazolol RMSD, Cmpd-15 RMSD	**S1**(~1.0Å, ~2.0Å)
$\alpha_{1B}AR$-Cmpd-15		**S2**(~1.0Å, ~4.0Å) **S3**(~3.0Å, ~6.5Å) **S4**(~4.5Å, ~5.0Å)
$\alpha_{2A}AR$-Cmpd-15		**S3**(~2.3Å, ~6.0Å)
$\alpha_{2C}AR$-Cmpd-15		**S2**(~1.7Å, ~2.5Å) **S3**(~2.3Å, ~5.7Å) **S4**(~5.1Å, ~4.0Å)
β_1AR-Cmpd-15		**S1**(~0.8Å, ~2.0Å)
M_2R-LY2119620	Iperoxo RMSD, LY2119620 RMSD	**S1**(~2.0Å, ~2.0Å) **S2**(~2.0Å, ~5.5Å)
M_4R-LY2119620		**S3**(~0.8Å, ~4.0Å) **S4**(~0.8Å, ~7.5Å)
M_1R-LY2119620		**S2**(~1.5Å, ~6.0Å)
D_1R-LY3154207	SKF-81297 RMSD, LY3154207 RMSD	**S1**(~1.5Å, ~1.5Å)
D_2R-LY3154207		**S2**(~3.0Å, ~15.5Å) **S3**(~3.0Å, ~11.5Å)